

# SOHO UVCS AND MAUNA LOA MARK IV OBSERVATIONS OF A SLOW CME BELOW 2 SOLAR RADII

A. Bemporad<sup>1</sup>, G. Poletto<sup>1</sup>, and J. C. Raymond<sup>2</sup>

<sup>1</sup>INAF–Arcetri Astrophysical Observatory, L.go E. Fermi 5, 50125 Firenze, Italy

<sup>2</sup>Harvard–Smithsonian Center for Astrophysics, 60 Garden Street, Cambridge, MA 02138

## ABSTRACT

In this work we study the early evolution of a slow (500 km/s) CME that occurred on January 31, 2000, and was observed by UVCS at 1.6 and 1.9  $R_{\odot}$ . The whole event turns out to be very faint in UV line emission: different CME structures are hardly identifiable in all the main spectral lines we detected ( $\text{Ly}\alpha$ , O VI and Si XII) whose intensities show during the event only a decrease by about 30–40% with respect to the value at the beginning of the observations, followed by some fluctuations. Taking advantage of the Mauna Loa white light data, we identified in the UV intensities the emission from the typical three parts (front, void and core) of our CME, rarely observed at these low altitudes. From the Mauna Loa  $pB$  data we estimated the electron densities in the different parts of the CME and, by assuming a simple geometry for the CME bubble, we derived an order of magnitude estimate of its mass. Taking advantage of densities we derived from the  $pB$  (hence, independently of the unknown plasma temperature), we qualitatively discuss the possible temperature variations across the CME bubble needed to reproduce the observed  $\text{Ly}\alpha$ , O VI and Si XII line intensity evolution. In particular, temperature changes at the CME core seems to be confirmed by the variations of the O VI  $\lambda$  1032 Å line widths observed at both heliocentric distances in this part of the CME bubble.

Key words: Sun: coronal mass ejections (CMEs) – Sun: UV radiation.

## 1. INTRODUCTION

Despite the large amount of UV and white light (WL) observations of Coronal Mass Ejections (CMEs), there are still many open questions about these phenomena: first, their real nature and cause are at present not completely known and for this reason the studies of physical conditions at the CMEs source regions and of the surrounding coronal magnetic field configurations are particularly important. Second, because of projections along the line of sight (LOS) and of the optical thinness of coronal plasmas, the real CME 3D geometry is still unknown (the fu-

ture STEREO mission will probably help us to solve this problem). Third, there are few simultaneous observations of CMEs in UV and WL intensities, hence the temperature structure within the expanding bubble is at present not completely known; moreover, because these observations are often made above the LASCO/C2 occulting edge (hence above 2  $R_{\odot}$ ), the early evolution of CMEs is not well studied.

Previous observations often revealed the CME core to be visible in spectral lines from ions which form in a low temperature plasma ( $\sim 10^4$  K, see e.g. Ciaravella et al. (1997); Ventura et al. (2002)), but recent observations detected also a higher temperature emission ( $T > 1.6 \cdot 10^6$  K) in the CME void and at the top of the prominence core (Ciaravella et al., 2003). However UV observations are sometimes ambiguous, the plasma temperature cannot be firmly established and there are few studies on possible plasma heating sources within CMEs (see e.g. Akmal et al. (2001)).

In this work we analyze the early stages of a CME that occurred on January 31, 2000, for which we have data acquired simultaneously in WL (by the Mauna Loa Mark-IV coronagraph) and UV (by the SOHO/UVCS instrument) covering the first hours of the CME evolution. In § 2 we describe the morphology of our event as observed by Mark-IV and we explain how we estimate from  $pB$  data the CME mass and density. In § 3 we describe the observed evolution of the UV line intensities and we discuss temperature variations across the CME bubble; in § 4 we present our conclusions.

## 2. MAUNA LOA MARK-IV DATA

On January 31, 2000, the two LASCO (*Large Angle and Spectrometric Coronagraph*, see Brueckner et al. (1995)) C2 and C3 instruments aboard the SOHO satellite observed a CME in the NE quadrant at an approximate latitude of  $\sim 62^{\circ}\text{N}$ , which propagated in the outer corona at a speed of  $\approx 500$  km/s with (above the LASCO/C2 occulter height) a negligible acceleration<sup>1</sup>. This event, not

<sup>1</sup>See the LASCO CME catalog available on [http://cdaw.gsfc.nasa.gov/CME\\_list/](http://cdaw.gsfc.nasa.gov/CME_list/)

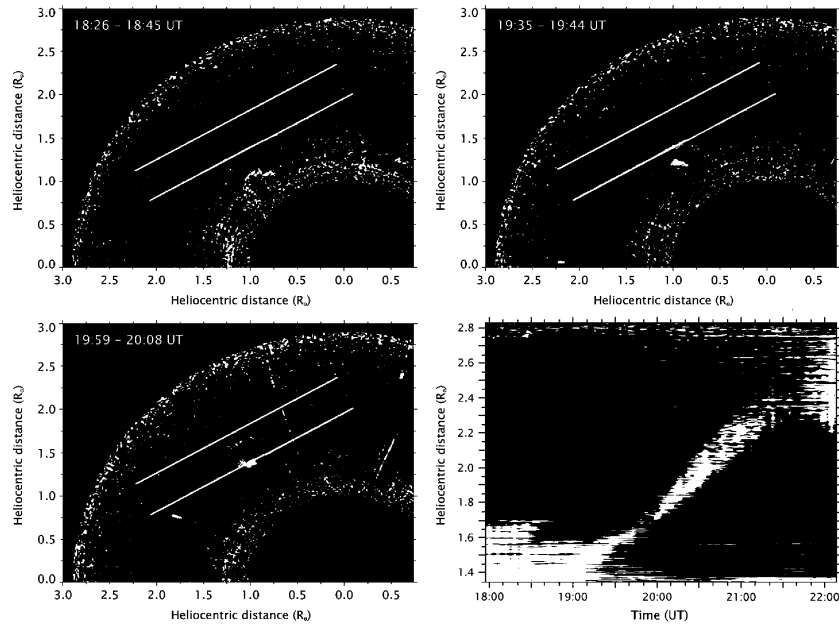


Figure 1. Top row and bottom left: a sequence of three Mauna Loa difference images (built from images acquired at the times given in each panel) showing the complex structure of the rising CME and the position of the UVCS slit at 1.6 and 1.9  $R_{\odot}$ . Bottom right: altitude vs. time profile of the CME intensity (from Mauna Loa Mark IV data) integrated over the CME latitudes.

associated with filament eruptions (as shown by the H- $\alpha$  images of the solar disk acquired by the Mauna Loa Observatory) or flares (as revealed by the GOES data), at least in the visible solar hemisphere, can be classified as a slow CME. On the same day, between 17:30 and 22:07 UT the Mauna Loa Mark-IV coronagraph (hereafter MKIV) acquired images of the low corona polarized brightness ( $pB$ ) from  $\sim 1.12$  to  $\sim 2.79 R_{\odot}$ <sup>2</sup>. As it is shown in Fig. 1, this time interval allows us to observe the early evolution of the event: in particular in the running difference images<sup>3</sup> it is possible to clearly identify the typical CME three-part structure, i.e. the CME front, void and core. Superposed onto these images we show, for future reference, the position of the UVCS slit (see § 3): because of the simple projected CME geometry, we expect to be able to distinguish in the UV spectra the emission from the different CME parts and derive informations on the plasma temperature.

In the bottom right panel of Fig. 1 we show the height vs. time CME curve; this has been built from the  $pB$  data acquired by MKIV by integrating in each exposure the observed intensity over the CME latitudes and subtracting the average coronal intensity in the whole dataset. The resulting image shows the presence of different CME substructures expanding at different speeds; analogous variations in the rising speed of different parts of a CME has been found, e.g., by Lin et al. (2005). From these curves

we derived that the motion of the CME front can be approximated by a constant acceleration of  $(34 \pm 4) \text{ m s}^{-2}$  starting from an heliocentric distance of  $\sim (1.5 \pm 0.8) R_{\odot}$  at  $\sim 18:13$  UT, while the CME core rises at a constant speed with a large spread of values between 70–100 km/s and no significant acceleration. The secondary substructures in between the accelerating CME front and the core seem to move at intermediate speeds. The evaluation of these velocities will be mandatory in order to reproduce the UV line intensities (see § 3).

Starting from the  $pB$  values observed at the CME front, void and core we estimate the electron density  $n_e$  as follows: first, we assumed a radial profile  $n_e(r)$  which, integrated along the LOS, reproduces the observed background  $pB$  (in particular, the Guhathakurta & Holzer (1994) profile multiplied by a constant factor of 6). Then we derived the additional density  $\bar{n}_e$  (representative of the CME density) needed to reproduce the observed  $pB$  at CME latitudes (and assuming the CME extension  $L$  along the LOS to be equal to its extension projected on the plane of the sky). Results from this technique are given in Fig. 2 (top left panel): by assuming  $L = 1 R_{\odot}$  we derived that at 1.6  $R_{\odot}$  the transit of the CME front, void and core corresponds to an increase (with respect to the average background density  $n_e(\text{cor}) = 7.4 \cdot 10^6 \text{ cm}^{-3}$ ) respectively by 35%, 27% and 50%.

By assuming a simple geometry for the structure of the whole CME bubble we derived from the above density values an order of magnitude estimate of the CME mass. In particular, by assuming for the CME geometry a cylin-

<sup>2</sup>See Mauna Loa movie at <http://mlso.hao.ucar.edu/>

<sup>3</sup>The transit of the CME is hardly identifiable in regular images because the CME WL emission is relatively faint with respect to the coronal background.

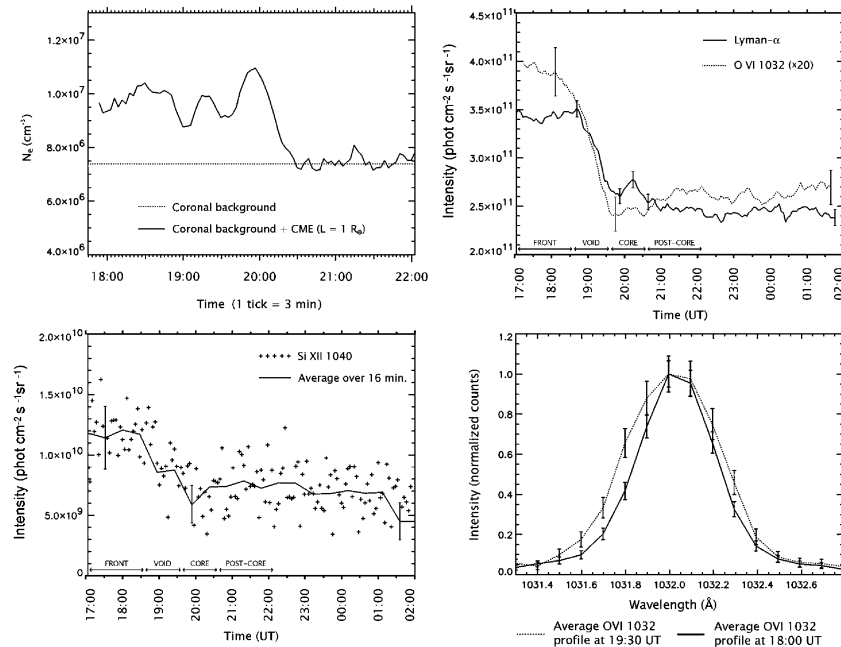


Figure 2. *Top left: the background plus additional electron density (solid) computed from the Mark IV  $pB$  data as a function of time averaged over the CME latitudes. Top right: the  $Ly\alpha$  and  $O\ VI\ 1032$  intensity evolution averaged over  $10^\circ$  around a latitude of  $50^\circ N$ . Bottom left: same as top right for the  $Si\ XII\ 1040$  line. Bottom right: a comparison between the normalized  $O\ VI\ 1032$  line profiles at two different times (averaged over 4 spatial bins around the latitude of  $\simeq 50^\circ N$  and 4 exposures) showing a  $\sim 25\%$  line broadening at the CME core.*

drical core extending over a depth of one solar radii along the LOS surrounded by two semicircular sheaths (core radius on the order of  $\sim 0.1 R_\odot$ ), the total CME mass is on the order of  $7 \cdot 10^{14} g$  at  $1.6 R_\odot$ . This mass (which resides mostly in the CME front surrounding the core) is about 1/3 of the CME final mass as measured by the LASCO/C3 images and reported in the LASCO CME catalog. Interestingly, by applying the same technique at  $1.9 R_\odot$  we derived that, taking into account the increase in the CME volume, the total mass increased by about a factor 2.6, hence at this altitude we found the CME mass to be about 90% of its final value.

Opposite to what happens when the electron densities are derived from an analysis of UV data, the above estimates have the advantage that are independent of plasma temperatures. In § 3 we discuss how, starting from the above density values, we give an estimate for the CME plasma temperature which allows us to reproduce the observed evolution of the UV line intensities.

### 3. SOHO UVCS DATA

The *UV Coronagraph Spectrometer* (UVCS, see Kohl et al. (1995)) observations started on January 31, 2000 at 17:05 UT and ended on February first at 02:00 UT. The UVCS slit was centered at a Northern latitude of  $60^\circ$  in the East quadrant (see Fig. 1) and two observation heights

have been used,  $1.6$  and  $1.9 R_\odot$ : the instrument took alternatively 12 exposures at  $1.6$  and 3 exposures at  $1.9 R_\odot$  (with an exposure time of 120 s), hence we have nearly “simultaneous” observations of the same event at two different altitudes.

The most intense spectral lines included in the selected spectral ranges are the hydrogen Lyman- $\alpha$   $\lambda$  1216 Å, the  $O\ VI\ \lambda\lambda$  1032–1037 Å doublet and the  $Si\ XII\ \lambda$  1040 Å (second order). Because during the transit of the CME we did not observe any significant line Doppler shift, we assume that the CME is propagating mainly in the plane of the sky.

In Fig. 2 we show the observed temporal evolution of the intensities of these lines averaged over the latitudes of the CME core. These plots show that, while the observed  $pB$  (hence the CME density) peaks at the CME core, the  $Ly\alpha$ ,  $O\ VI$  and  $Si\ XII$  line intensities peak at the CME front; moreover the CME core, observed in the  $Ly\alpha$  line, has no significant emission in the  $O\ VI$  and  $Si\ XII$  lines. The observed emission of the  $Ly\alpha$  and  $O\ VI$  lines in the solar corona can be due both to the excitation by collisions with thermal electrons or by the resonant scattering of photons emitted by the underlying levels<sup>4</sup>. In order to reproduce the observed UV line emission, it is mandatory to take into account that the radiative component can be reduced by the Doppler dimming effect (because of

<sup>4</sup>As we verified from the observed  $Ly\beta / Ly\alpha$  ratio, the  $Ly\alpha$  emission we detected is due only to the radiative excitation.

the radial component of the plasma outflow velocity, the atomic absorption profile is Doppler-shifted with respect to the emission profile and the radiative excitation process is less efficient).

At the CME front, taking into account the Doppler dimming factors we derived for the observed CME outflow speed and using the density value we derived from the  $pB$  data, the observed line emission is well reproduced by a plasma temperature of  $T = 10^{6.3}$  K. On the contrary, the Doppler dimming is not sufficient to explain the lack of  $\text{Ly}\alpha$  and  $\text{O VI}$  emission at the CME core. Moreover, the  $\text{Si XII}$  line intensity (which is due only to collisional excitation, hence it is not affected by Doppler dimming) does not maximize at the CME core, while from the density increase we should expect an intensity increase by a factor  $\sim 2.25$  with respect to the background emission. We conclude that the line intensity decrease from the CME front to the core shown in Fig. 2 can be explained only taking into account also a temperature increase. Because the  $\text{Si XII}$  line emissivity peaks<sup>5</sup> at a temperature of  $\log T = 10^{6.3}$ , we expect at the core a temperature larger than this value. This behaviour has been confirmed also by the analysis of UVCS data acquired at  $1.9 R_{\odot}$ .

The temperature increase at the CME core is further supported by the  $\text{O VI}$  1032 line profiles (Fig. 2, bottom right panel): the kinetic temperatures we derived from the line profile Gaussian fits are on the average  $\sim 25\%$  larger in the CME core region than in the CME front, as shown in Fig. 2. Larger temperature variations in the CME regions may be hidden in the average coronal plus CME line profile. We note that the observed line broadening can be due also to the plasma bulk motions along the LOS related to the CME expansion: between  $1.6$  and  $1.9 R_{\odot}$  the CME expands by about  $30\%$  and this corresponds to a bulk velocity of  $\pm 50$  km/s along the LOS, hence a Doppler shift of  $\pm 0.17$  Å which can possibly explain the observed line broadening; however, we are at present unable to distinguish between these two possibilities.

#### 4. CONCLUSIONS

In this work we studied the early evolution of a CME which occurred on January 31, 2000, with the aim of inferring the physical parameters of the CME front and core in the early stage of its development. From the  $pB$  data we derived the electron densities in the CME three part structures: their  $pB$  contrast with respect to the background has been reproduced by increasing the electron densities by  $35\%$  and  $\sim 50\%$  over the average background coronal density respectively for the CME front and core. From these values, by assuming a simple CME geometry, we computed that at  $1.6$  and  $1.9 R_{\odot}$  the CME mass is, respectively, about  $30\%$  and  $90\%$  of its total mass as derived at higher levels from LASCO/C3 images. As

<sup>5</sup>In this work we used the line emissivities given by the CHIANTI spectral code v.5 with the ionization equilibrium of Mazzotta et al. (1998).

pointed out by Lin et al. (2004), the mass of a CME increases with increasing heliocentric distances, because of the progressive reconnection of new fieldlines around the CME bubble. Hence, our results are at least in qualitative agreement with the Lin et al. (2004) scenario.

An interesting result we derived is the temperature variation across different CME structures, in particular a temperature higher by a factor 2.0 than the surrounding  $1.4 \cdot 10^6$  K corona in the CME core. This result is opposite to what envisaged by the Lin et al. (2004) model where plasma in the outer layers of the CME bubble, being the latter to reconnect at the top of the current sheet, is expected to be hotter (i.e. temperatures decrease from the external bubble shells towards the CME core). The behaviour we inferred may be explained if the heating provided by the magnetic energy dissipation during the CME expansion is larger than the plasma cooling due to the adiabatic expansion. However further analysis of this problem is needed.

#### ACKNOWLEDGEMENTS

This work initiated during a visit of A.B. to the Harvard-Smithsonian Center for Astrophysics whose hospitality and support is gratefully acknowledged. A.B. and G.P. acknowledge support from ASI-INAF contract I/035/05/0. SOHO is a mission of international cooperation between ESA and NASA.

#### REFERENCES

- Akmal, A., Raymond, J.C., Vourlidas, A., et al. 2001, *ApJ*, 553, 922
- Brueckner, G.E., Howard, R.A., Koomen, M.J., et al. 1995, *SP*, 162, 357
- Ciaravella, A., Raymond, J.C., Fineschi, S., et al. 1997, *ApJ*, 491, L59
- Ciaravella, A., Raymond, J.C., van Ballegooijen, A., et al. 2003, *ApJ*, 597, 1118
- Guhathakurta, M., & Holzer, T.E. 1994, *ApJ*, 426, 782
- Kohl, J.L., Esser, R., Gardner, L.D., et al. 1995, *SP*, 162, 313
- Lin, J., Raymond, J.C., & van Ballegooijen, A.A. 2004, *ApJ*, 602, 422
- Lin, J., Ko, Y.-K., Sui, L., et al. 2005, *ApJ*, 622, 1251
- Mazzotta, P., Mazzitelli, G., Colafrancesco, S., & Vittorio, N. 1998, *A&AS*, 133, 403
- Ventura, R., Spadaro, D., Uzzo, M., & Suleiman, R. 2002, *A&A*, 383, 1032